The Structure and Reactivity of Al_2O_3-Supported Cobalt−Palladium Particles: A CO-TPD, STM, and XPS Study

A. F. Carlsson,* M. Naschitzki, M. Bäumer, and H.-J. Freund

Fritz-Haber-Institut der Max-Planck-Gesellschaft, Department of Chemical Physics, Faradayweg 4-6, 14195 Berlin, Germany

Received: August 27, 2002; In Final Form: October 25, 2002

Bimetallic Co−Pd Fischer−Tropsch catalysts have shown increased activity toward CO-hydrogenation and methane conversion. A model for these Fischer−Tropsch catalysts has been constructed and studied under ultrahigh vacuum conditions. The morphology, growth modes, exposed binding sites, and electronic properties of Co−Pd bimetallic particles supported on a thin alumina film have been studied using scanning tunneling microscopy (STM), temperature-programmed desorption (TPD) of CO, and X-ray photoelectron spectroscopy (XPS). Sequential deposition of Co and Pd results in a core−shell structure. Three-fold hollow sites are easily dismantled, whereas atop sites are statistically resilient upon the formation of a bimetallic shell. The binding energy of CO to each of the metals is lowered by the presence of the other. A shift in the Pd 3d level to higher binding energy concurrent with a shift in the Co 2p level to lower binding energy suggests a net polarization of charge or redistribution of d-band states.

Introduction

The changing availability of natural resources and an increasing demand for cleaner fuels solicits a better understanding of the catalytic processes for the conversion between the two. Synthesis gas ($CO + H_2$) produced from coal, natural gas, oil, or biomass can be used to produce methanol using the Fischer−Tropsch reaction,[1] for which a combination of oxide-supported transition metals is often used. For example, the addition of Pt or Pd to Fe or Co catalysts has been shown to increase the selectivity for methanol formation from synthesis gas at high pressure.[2−5] The conversion of methane to higher hydrocarbons[6] and hydrogenation of CO[7−9] show higher conversion and selectivity on Co−Pd bimetallic supported catalysts than either metal alone. To understand the changes in reactivity affected by a second metal component in a catalyst, we took up a fundamental study of Co−Pd bimetallic particles supported on NiAl(110)−Al_2O_3. Inspired by the earlier work of Henry and co-workers,[10,11] different structures and compositions were prepared by taking advantage of the nucleation and growth properties of the two metals.

Supported bimetallic Co−Pd catalysts have previously been studied in non-UHV conditions.[6−9,12−21] It has been proposed that the addition of Pd promotes the reduction of Co oxide by activating hydrogen.[6−9,16−19,21] Magnetic measurements[19] and temperature-programmed reduction[9] have shown that CoO is more easily reduced when Pd is added as a cocatalyst.

In general, the addition of a second metal as a cocatalyst affects both electronic and structural changes in the original catalyst. For example, when CO is atop bonded on a Pd atom surrounded by gold atoms, the binding energy is 68.5 kJ/mol; in contrast, when the Pd atom is surrounded by other Pd atoms, the binding energy of atop-bound CO is 73.3 kJ/mol.[22−24] This difference in binding energy induced by the electronic interaction of the two metals is termed a ligand effect.[25] On one hand, the ligand effect can be viewed as a polarization of charge[26] or a charge-transfer effect. On the other, DFT calculations show that a compression or rarefaction of the metal lattice due to pseudomorphic growth affects a change in adsorbate binding energy through a shift in the center of gravity of the d-band.[27] Experiments have shown[28] that bimetallic growth is usually pseudomorphic when the lattice mismatch is less than ∼7−9%, above which an incommensurate structure forms. The lattice mismatch for Pd−Co is about 10%.

Further, the availability of binding sites for adsorbates may change when a second metal component is added. For example, if CO would prefer to bind in 3-fold Pd hollow sites, but every other Pd atom is substituted for Au, the CO may be forced to bind at a bridge or atop site. For example, the binding energy of atop-bound CO to a Pd atom surrounded by Au atoms is 68.5 kJ/mol, whereas the binding energy of 3-fold-hollow-bound CO to 3 Pd atoms surrounded by Au atoms is 107.1 kJ/mol.[24] Indeed, CO does prefer 3-fold hollow sites over atop sites on the pure Pd(111) surface as well.[29] For the example of CO adsorption on the Pd−Au system, the structural effects (107.1 kJ/mol vs 68.5 kJ/mol) are much more pronounced than the electronic effects (73.3 kJ/mol vs 68.5 kJ/mol).[22−24]

In this study, CO is used as a probe molecule for investigating the properties of supported bimetallic Pd−Co clusters; thus a brief background on the adsorption of CO on the pure metal single crystals is necessary. CO preferentially occupies fcc 3-fold hollow sites ($\theta < 0.33$ ML) on Pd(111),[30] from which the effective desorption energy is 35.5 kcal/mol and the preexponential factor is $10^{13.5}$ s^{-1} ($T_d \sim 445$ K).[29] At higher coverages ($\theta \sim 0.50$ ML), CO occupies fcc and hcp 3-fold sites[30] on Pd(111), from which the effective desorption energy is 17.3 kcal/mol and the preexponential factor is about $10^{2.7}$ s^{-1}.[29] At higher coverages ($\theta = 0.6-0.7$ ML), bridge sites are occupied ($T_d \sim 310$ K).[31] Finally, at the highest coverage obtainable under UHV conditions ($\theta = 0.75$ ML), CO occupies atop and 3-fold sites[31] on Pd(111) from which the effective desorption energy is about 11 kcal/mol and the preexponential factor is about $10^{2.7}$

* Author to whom correspondence should be addressed. Fax: +49 30 8413 4101. E-mail: carlsson@fhi-berlin.mpg.de.

10.1021/jp021966v CCC: $25.00
Published on Web 12/20/2002

s^{-1} ($T_d \sim 190$ K).[29] It is likely that the variation in the preexponential factor is due at least in part to the use of the rate equation as an overall description for a desorption process which may also be precursor-mediated.[29] Part of the drop in E_d may be due to lateral interactions,[29] but comparison with DFT calculations[27,32] shows that different sites have different binding energies in the absence of lateral interactions as well.

CO adsorbed on Pd particles on Al_2O_3/NiAl(110) shows slightly different behavior compared with that on the single-crystal Pd(111) surface.[33] At saturation coverage, CO binds to atop, bridge, and 3-fold hollow sites, whereas on the Pd(111) surface, the bridge-sites vanish at saturation coverage. Both (111) and a minority of (100) facets are present on the supported Pd particles,[34] both of which adsorb CO. Higher-coordinated sites are populated before any atop sites are filled.[33]

Sum frequency generation (SFG) was used to probe CO adsorption on the Pd particles (3 and 6 nm mean size) at pressures up to 200 mbar.[35] At 300 K only bridge sites were detected (3-fold sites could not be monitored due to experimental limitations) at 10^{-7}mbar, but atop sites could be repopulated at pressures above 1mbar.[35] Atop sites could be populated at 190 K but not at 300 K with a background pressure of 10^{-7}mbar. Clearly, an analogy can be drawn to vapor−liquid equilibrium, where we would expect condensation to a higher density phase at higher pressures or lower temperatures. The CO-coverage dependence also depends on surface structure, particularly for smaller particles, which have a larger fraction of terminally bonded CO.[36]

CO preferentially binds to atop sites on the close-packed Co(0001) surface ($\theta < 0.33$ ML),[37] from which the effective desorption energy is about 27.4 kcal/mol (114.5 kJ/mol) with a preexponential factor of 10^{15} s^{-1} ($T_d \sim 400$ K).[38] At higher coverage ($\theta = 0.43$ ML), CO binds to bridge sites, from which the effective desorption energy is about 19 kcal/mol (75 to 82 kJ/mol) ($T_d \sim 320$ K).

The site-occupation of CO on Co(10−10) is similar to that on Co(0001). CO preferentially binds to atop sites on Co(10−10) at coverages below 0.5 ML, from which the desorption energy is 110.7 kJ mol^{-1} with a preexponential factor of 3.1×10^{13} s^{-1}.[39] At coverages between 0.5 ML and 1 ML, CO occupies 2-fold bridge sites between first layer Co atoms along the rows. CO molecules tilt in opposite directions due to the close packing, and desorption occurs at ∼340 K.[39] At coverages between 1 ML and 1.055 ML, there is a complex compression structure which desorbs at ∼232 K.[39] A later FTIR study revealed that at a coverage of 1.055 ML and surface temperatures between 150 K and 180 K, CO occupies both bridge and 3-fold sites.[40] No CO dissociation was found on Co(10−10),[39] in agreement with earlier studies.[41]

The primary practical motivation for the current study is that Pd promotes both methane activation and CO hydrogenation over a Co Fischer−Tropsch catalyst; a fundamental motivation is the difference in CO binding morphology on Pd and Co. Generally, CO seems to prefer the atop site on transition metals, to which the Ni−Pd−Pt group is an exception.[37] Ensemble and electronic effects in CO adsorption may differ when either Pd or Co is the dominant component due to the 3-fold preference on Pd and the atop preference on Co.

Experimental Section

The experimental apparatus used in this study has been described in detail elsewhere.[42] Briefly, it consists of a commercially built analysis chamber (Omicron) with an AFM/STM stage, as well as XPS and LEED. Coupled to the analysis chamber by a transfer system is a preparation chamber containing Pd and Co metal evaporators, and facilities for sputtering, gas dosing, and TPD measurements. The base pressures in the analysis and preparation chambers are 1×10^{-11} mbar and 1×10^{-10} mbar, respectively. The metal evaporators were calibrated both with a quartz micro-balance in a different chamber and the STM in the analysis chamber. The average thickness of the film is herein given in Ångstroms, where 1 ML is equivalent to 2.035 Å Co or 2.246 Å Pd. The NiAl(110) crystal was cleaned by cycles of Ar^+ sputtering, and an Al_2O_3 film was prepared by previously described methods.[33,43] STM measurements were taken at tip biases of 5−6 V and tunneling currents of 0.1 to 0.2 nA. All STM images were subject to plane or slope background subtraction and adjustment of color contrast. XPS measurements were taken at pass energies of 25 eV with 20 sweeps.

During TPD measurements, the sample was exposed to CO through a directed doser at 100 K and then placed less than 1 mm away from the differentially pumped cap of the quadropole mass spectrometer. The sample was heated by radiation from a tungsten filament mounted directly behind it. The temperature ramp was accurately programmed with a controller and power supply from H. Schlichting. Blank TPD measurements from the oxide film without deposited metal particles showed that desorption of small amounts of masses 2, 16, 18, 28, 32, and 44 below 150 K were due to desorption from the heating filament; these signals were at least an order of magnitude smaller than those resulting from desorption from the metal particles. We also noted that a background dose of CO (keeping the sample temperature constant) caused masses 28, 44, and 16 to appear in the mass spectrum, indicating some reaction in the region of the hot filament. The ratio of these signals was noted for comparison when looking for reactions of CO on the metal particles during TPD. The alumina film does not show adsorption of CO above 90 K.[44]

Results and Discussion

1. STM. STM images show that at 300 K the majority of Pd particles nucleate and grow at antiphase and reflection domain boundaries on the alumina film.[33] Closer inspection of the triangular-shaped Pd particles has shown the sides and top to be formed by (111) faces.[34] In contrast, pure Co nucleates at point defects on the alumina film under these conditions, as shown by STM.[45,46] At temperatures above 300 K, where Co atoms on the surface are more mobile, nucleation increasingly occurs at line defects;[47] in general, Co atoms are less mobile than Pd atoms on the alumina substrate due to a stronger metal−substrate interaction.[47]

STM images show that evaporated Pd metal preferentially nucleates on Co particles previously deposited on the alumina surface. The notation "2 Å Co + 1 Å Pd" will be used as shorthand for first deposition of 2 Å Co, then subsequent deposition of 1 Å Pd; all metal deposition was done at 300 K. STM images taken after TPD measurements (Figure 1) show similar particle density for 2 Å Co with varying amounts of Pd. This clearly shows that Pd prefers to nucleate at the Co particles already present on the surface. The TPD results presented below suggest that the Pd forms a shell-structure on top of the Co particles. STM images taken on the pristine surfaces and ones annealed to 530K during TPD were similar.

The growth of the core−shell structure of Co−Pd particles roughly follows the original three-dimensional shape of the pure Co particles. An STM image of the 2 Å Co + 0.1 Å Pd particles looks qualitatively similar to the STM images of 2 Å Co + 1

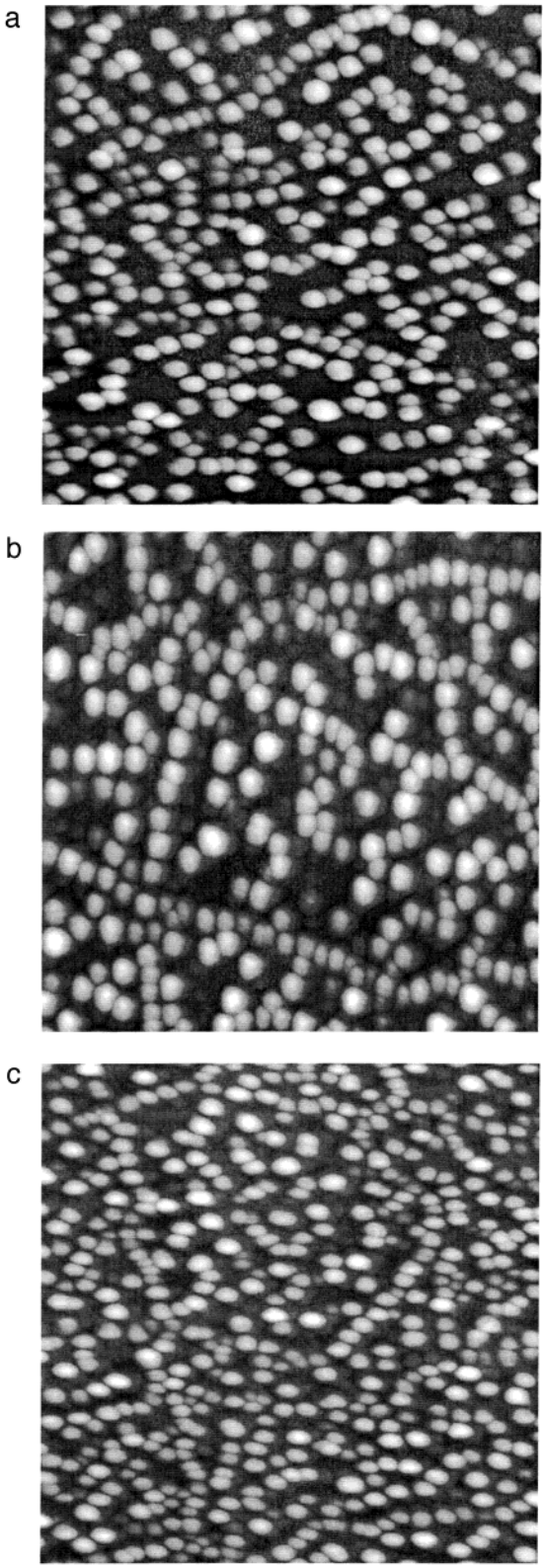

Figure 1. 100 nm × 100 nm STM images of (a) 2 Å Co and subsequently 0.1 Å Pd, (b) 2 Å Co and subsequently 1 Å Pd, and (c) 2 Å Co and subsequently 2 Å Pd deposited on the alumina film at 300 K taken after a TPD measurement.

Å Pd or 2 Å Co + 2 Å Pd (Figure 1). Further, the particle heights estimated from STM are 2.7 nm, 2.7 nm, and 3.0 nm, respectively, for the three surfaces, while the particle diameter is about 3 nm in all cases; the measured particle diameter is about double this value due to tip convolution effects.[48]

The thickness of Pd needed to fully cover the Co particles can be calculated from the overall shell thickness and the particle diameter. The average thickness of Co deposited is calibrated with a quartz microbalance, and the particle density can be estimated from STM images. Assuming that a shell of Pd atoms one atom thick (2 Å) coats hemispherical Co particles and does not inter-mix, we would expect 1.2 Å of Pd to fully cover the 2 Å Co particles. The TPD results below show that indeed CO desorption from Pd 3-fold sites is observed only at coverages higher than 1.2 Å Pd.

When Pd is deposited first, particles nucleate at steps and antiphase domain boundaries;[46] subsequent deposition of Co results in the Pd particles becoming covered with Co (shown by TPD below) as well as the nucleation of separate Co particles at point defects. Figure 2 shows an STM image of 2 Å Pd + 1 Å Co where large triangular-shaped particles which look similar to the particles of pure 2 Å Pd.[33] In addition, there are smaller round particles appearing to have nucleated at defects rather than at grain boundaries − characteristic of Co nucleation.

The amount of Co required to cover the Pd particles can be calculated from the overall shell thickness and the dimensions of the average Pd particle. The calculation in this case is a rougher approximation, because not all Pd particles on the surface form well-defined triangular crystallites. Furthermore, there is another degree of freedom in calculating the volume from the more complex geometry, so the height measurement must be taken from STM data. In addition, the small amount of Co nucleated between Pd particles is not counted. Modeling each particle as a vertically grown isosceles triangle we calculate that the average thickness of Co needed to coat the Pd particles is 1.44 Å. As we would expect, this is just slightly more than is required to coat the same volume of hemispherical particles. The effect of Co in the TPD measurements (discussed below) can be seen at coverages much lower than 1.44 Å; because CO adsorbs on the atop sites of Co, only a small number of Co atoms are needed to see an effect, in contrast to the 3-fold bound CO on Pd. It is possible that the amount of the second metal needed to coat the first is higher than estimated above; the second metal might not smoothly coat the first.

2. TPD. *2.1. Co Particles with Pd on Top.* (*a*) *Co Sites.* Each TPD spectrum shown in Figure 3 was taken after sequential deposition of Co and Pd on the Al_2O_3 film/NiAl(110) at a surface temperature of 300 K, and subsequent dosing of 20 L CO at 100 K. The surface was prepared anew for each TPD measurement. The bottom-most spectrum in the series shows TPD of CO from pure Co particles on the alumina film. In agreement with literature data from single-crystal studies,[38] we observe desorption from atop sites (393 K) and a smaller amount from bridge sites (278 K). The TPD spectrum of CO desorbing from 0.5 Å Co particles shows a higher population of atop sites relative to bridge sites compared with the TPD spectrum of CO desorbing from 2 Å Co particles (Figure 4). This is in agreement with similar observations for Pd particles.[33]

When 0.1 Å Pd is deposited on top of 2 Å Co (Figure 3), the CO desorption peak from Co-atop sites does not shift, but the desorption peak from Co-bridge sites shifts slightly to lower binding energies (labeled "B"). At 2 Å Co + 0.5 Å Pd and 2 Å Co + 1 Å Pd, the CO desorption peak from the Co-atop sites diminishes, while a new peak, labeled "A", grows in; we attribute this new peak to CO desorption from Co-atop sites which are neighbored by at least one Pd atom. At a coverage of 0.1 Å Pd, only a small portion of the Co atoms have neighboring Pd atoms, and the peak appears only as a small shoulder on the peak due to desorption from the Co-atop sites

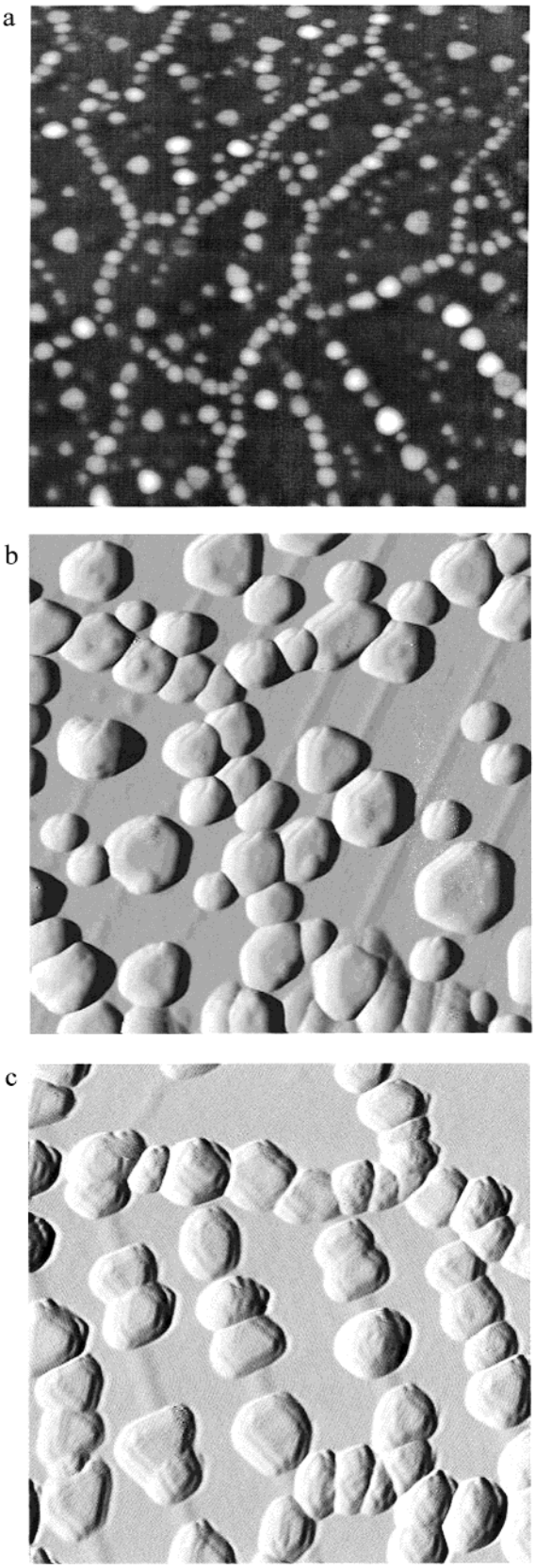

Figure 2. STM images of Pd and subsequent Co deposition at 300 K on the alumina film: (a) 100 nm × 100 nm image of 1 Å Pd and subsequently 0.5 Å Co (no TPD), (b) 50 nm × 50 nm image of 2 Å Pd and subsequently 1 Å Co (after TPD, differentiated to show contrast), and (c) 50 nm × 50 nm image of 2 Å Pd alone for comparison (differentiated to show contrast).

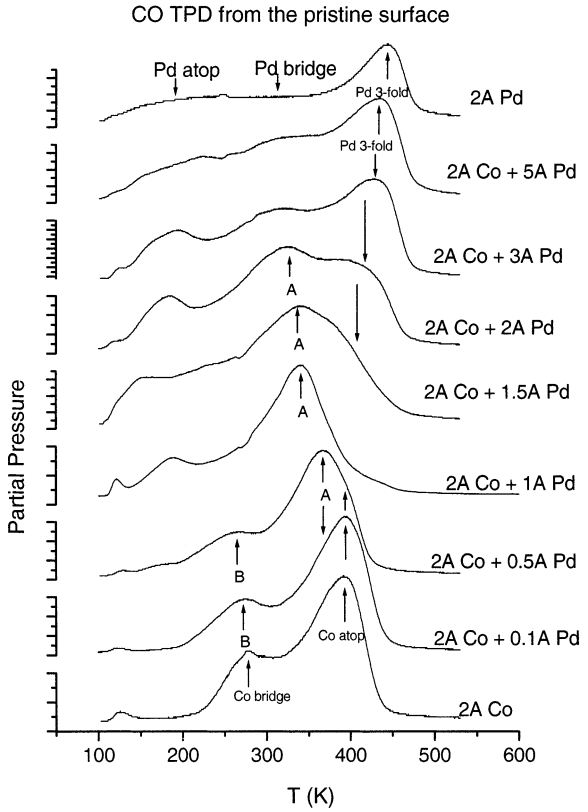

Figure 3. TPD spectra of CO from various pristine Co + Pd particles supported on Al_2O_3/NiAl(110). Metals were deposited at 300 K and 20 L CO were dosed at 100 K prior to TPD. The heating rate was 1.5 K s^{-1}.

bordered only by Co. In contrast, at 0.5 Å Pd coverage on top of 2 Å Co, there are probably more Co atoms having Pd-atom neighbors than those surrounded only by Co; thus, the peak "A" grows in strongly. When 1 Å Pd is added to the 2 Å Co particles, a strong peak arises which may be due to CO desorption from the same Co-atop sites, but this time where the Co atoms are surrounded by more neighboring-Pd atoms. As the amount of Pd-coverage on the 2 Å Co-particles increases, the CO-desorption peak from Co-atop sites continues to shift to lower binding energies, but then diminishes quickly at 3 Å Pd coverage, when the Co particles are fully covered by Pd.

The CO desorption peak from Co-bridge sites has been labeled "B" when it is shifted to lower binding energies due to the addition of 0.1 Å Pd (Figure 3). At 0.5 Å Pd coverage added to 2 Å Co, the "B" peak shifts to even lower binding energies, following the trend of the Co-atop bound CO. By the time 1 Å Pd is added to the 2 Å Co particles, the "B" peak has completely vanished, presumably because there are no more pure Co-bridge sites left. This is consistent with our previous assertion that the Co-atop sites are nearly surrounded by Pd at this coverage.

(*b*) *Pd Sites.* The highest-temperature peak for CO desorption from the pure Pd (2 Å) particles is at 444 K (Figure 3), in agreement with CO desorption from 3-fold hollow sites from the single-crystal Pd(111) surface.[29] On the single-crystal surface, desorption states from bridge and atop sites were also seen,[29] though they are not resolved in the TPD spectrum from the particles (Figure 3, top curve).

The binding sites of CO on alumina-supported Pd particles were determined with IRAS by annealing the CO-saturated sample to various temperatures.[49] Terminally bonded (atop) CO was observed with IRAS[49] up to 300 K, suggesting that part of the broad CO-desorption peak below 300 K is due to a

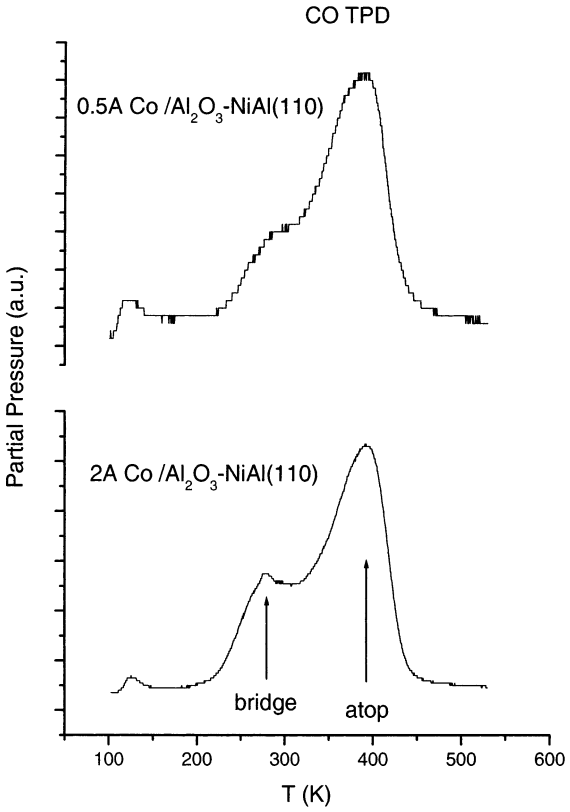

Figure 4. TPD spectra of CO from 0.5 Å and 2 Å Co particles supported on Al_2O_3/NiAl(110). Co was deposited at 300 K and 20 L CO were dosed at 100 K prior to TPD. The heating rate was 1.5 K s^{-1}.

depopulation of atop sites; this is in general agreement with single-crystal studies.[30] The desorption region for atop-bound CO is labeled in the top spectrum of Figure 3 for the pure Pd particles. Bridge-bonded CO was observed with IRAS[49] up to 370 K, suggesting that part of the broad CO-desorption peak just below 370 K is due to the depopulation of bridge sites; the desorption region for bridge-bound CO is correspondingly labeled in Figure 3. The desorption of CO from 3-fold hollow sites is assigned to the peak at 443 K (top spectrum, Figure 3), in agreement with the IRAS findings.[49]

When there is 2 Å of Co underneath 5 Å or 3 Å of Pd, the binding energy of CO in the 3-fold hollow site decreases with decreasing total amount of Pd; this decrease is most likely due to the electronic influence of underlying Co atoms (ligand effect) This ligand effect becomes stronger when there is a thinner layer of Pd shielding the topmost layer of Pd atoms from the underlying Co. At a coverage of 2 Å Pd on top of 1.5 Å Co, the number of available 3-fold sites quickly diminishes, resulting in the desorption feature becoming only a shoulder on the main spectrum.

2.2. Pd Particles with Co on Top. (*a*) *Pd Sites.* When Pd and Co are deposited on the alumina film in the reverse order, i.e., Pd first and subsequently Co, similar trends appear (Figure 5). The TPD spectrum of CO desorbing from pure 2 Å Pd particles is shown in the top panel of Figure 5 for comparison with the other spectra. When 0.1 Å Co is deposited on top of 2 Å Pd particles, the desorption temperature of CO from the 3-fold Pd sites is lowered from 444 K down to 417 K. When 0.5 Å is deposited on top of 2 Å Pd particles, the desorption of CO from 3-fold hollow sites is not observed at all, presumably because the Co efficiently obstructs the 3-fold Pd sites.

(*b*) *Co Sites.* The TPD spectrum of CO desorbing from pure 2 Å Co particles is shown in the bottom panel of Figure 5 for

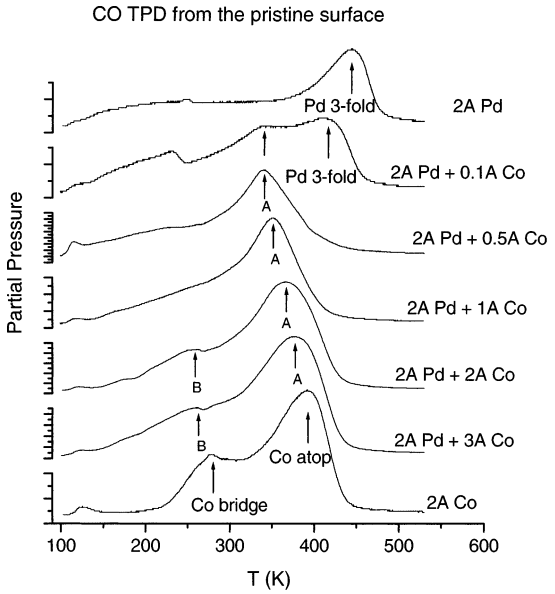

Figure 5. TPD spectra of CO from various pristine Pd + Co particles supported on Al_2O_3/NiAl(110). Metals were deposited at 300 K and 20 L CO were dosed at 100 K prior to TPD. The heating rate was 1.5 K s^{-1}.

comparison with the other spectra. When 3 Å Co is covering 2 Å Pd particles, the desorption peak of CO from Co-atop sites is shifted from 393 K down to 378 K. At thinner Co coverages on top of 2 Å Pd particles, the desorption temperature of CO from Co-atop sites continues to shift to lower temperature in a seemingly continuous fashion (Figure 5). Finally, at only 0.1 Å Co on top of 2 Å Pd particles, the CO desorption peak from Co-atop sites is at 341 K.

The TPD spectrum of CO desorbing from pure 2 Å Co particles (bottom panel Figure 5) also shows desorption of CO from bridge sites. When 3 Å or 2 Å Co is covering 2 Å Pd particles, the desorption of CO from the Co-bridge site shifts from 280 to 265 K and then to 260 K, respectively. At 1 Å Co coverage on top of 2 Å Pd, the peak due to CO desorption is gone, presumably because there are no Co-bridges remaining.

General Comments. The binding energy of CO to each of the metals is lowered by the presence of the other. When Pd is deposited on top of Co particles, the desorption temperature of CO on Co-atop sites is lowered from 393 K to 327 K, and the desorption temperature of CO in Pd 3-fold sites is lowered from 444 K to 408 K. When Co is deposited on top of Pd particles, the desorption temperature of CO on Co-atop sites is lowered from 393 K to 341 K, and the desorption temperature of CO in Pd 3-fold sites is lowered from 444 K to 417 K. It is likely that the limit of the binding energy shift of CO is not dependent on whether Pd or Co is deposited first, though ensemble (structural) effects do not allow the exact limits to be measured. Roughly speaking, the binding energy of CO to the Co-atop site is lowered by 19.3 kJ/mol by the presence of neighboring Pd atoms, and the binding energy of CO to Pd 3-fold sites is lowered by 9.6 kJ/mol by the presence of neighboring Co atoms.

When bimetallic particles are formed, the 3-fold sites are first to disappear. Statistically, this makes sense because a greater degree of order and freedom from contamination by a second metal is required. For example, the Pd 3-fold sites disappear when less than 0.5 Å (0.25 ML) of Co is added on top of the 2 Å Pd particles. In contrast, Co-atop sites survive on 2 Å Co particles even when up to 3 Å Pd is deposited on top of the original Co particles. Thus, we expect that the reactivity of atop sites will be better preserved in our system than the reactivity

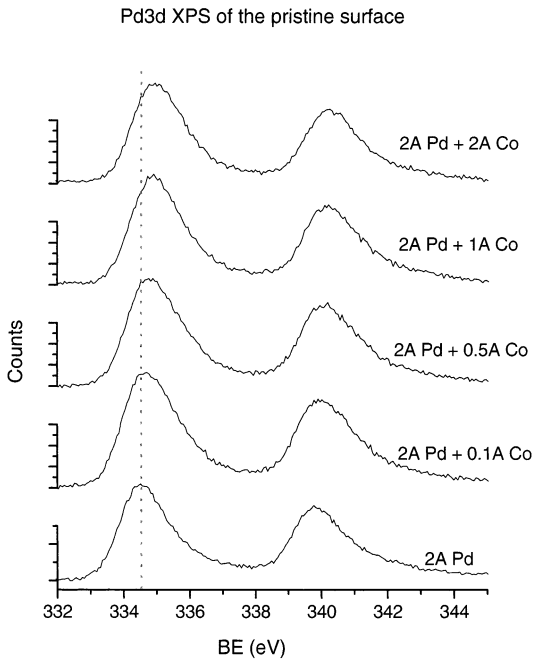

Figure 6. XPS spectra of the Pd 3d level at various Co-shell coverages on an original 2 Å Pd.

of 3-fold sites. The bridge sites are an intermediate case: they are not as fast to disappear as the 3-fold sites, but are also not as persistent as the atop sites upon bimetallic formation.

Because only one atom is required for an atop site, a small number of atop-binding atoms can affect a large change in the reactivity of bimetallic particles. At only 0.1 Å Co coverage on top of 2 Å Pd particles, there is a significant amount of CO adsorption on Co-atop sites compared with that on Pd 3-fold sites (Figure 5); in contrast, at 0.1 Å Pd on top of 2 Å Co particles, the CO adsorption behavior appears the same as on the pure Co particles (Figure 3). Certainly some of the Pd 3-fold sites are destroyed because Co atoms sit on top of them or displace one of the Pd atoms in the trio; however, it is also possible that Co adatoms disrupt the packing of the Pd trio enough to affect a change in their interaction with CO.

3. XPS. Figures 6 and 7 show XPS spectra of the Pd 3d and Co 2p levels for various Co-shell coverages on top of 2 Å Pd. Beginning at 0.1 Å Co, there is a slight shift in the Pd 3d level to higher binding energy, increasing with Co coverage (Figure 6). The maximum shift of 0.4 eV is reached at a shell thickness of 1 Å Co, and does not change as the Co shell thickness is further increased to 2 Å Co. The shift in the Pd 3d binding energy with increasing Co coverage is somewhat unexpected, since we would not expect all the atoms in the Pd particle to be affected equally by a small addition of Co. Pd particles deposited at 90 K, which are not as well ordered as those deposited at 300 K,[47] also show a similar shift in binding energy when a Co shell is added. At 0.1 Å Co coverage, the Co 2p level is shifted to lower binding energy by 2.2 eV relative to the pure Co particles (Figure 7). At higher Co coverages, a smaller shift is observed, until at 2 Å Co, the Co 2p binding energy is the same as it is on the pure Co particles. The influence of the underlying Pd core is greatest on a smaller number of Co atoms in the shell.

Similar shifts have been observed for Co−Pd bimetallic catalysts prepared by the sol−gel method[9] and impregnation.[8] Theoretical studies indicate that the bimetallic bond is best described as metallic with a small degree of ionic character.[50] Theoretical calculations also show that a rehybridization of

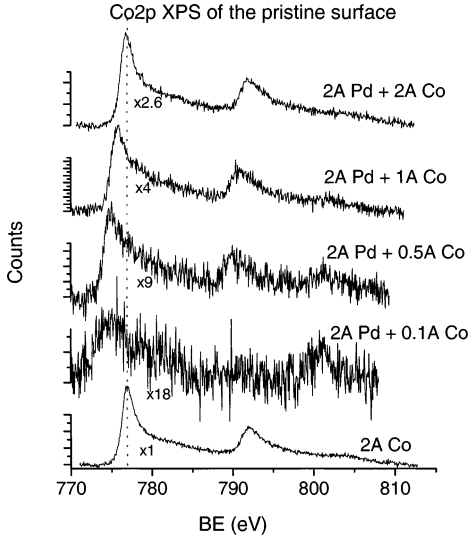

Figure 7. XPS spectra of the Co2p level at various Co-shell coverages on an original 2 Å Pd. The small peak appearing at 803 eV is an x-ray satellite from a Ni peak, and also appears in the spectrum of the clean film without any deposited Pd or Co.

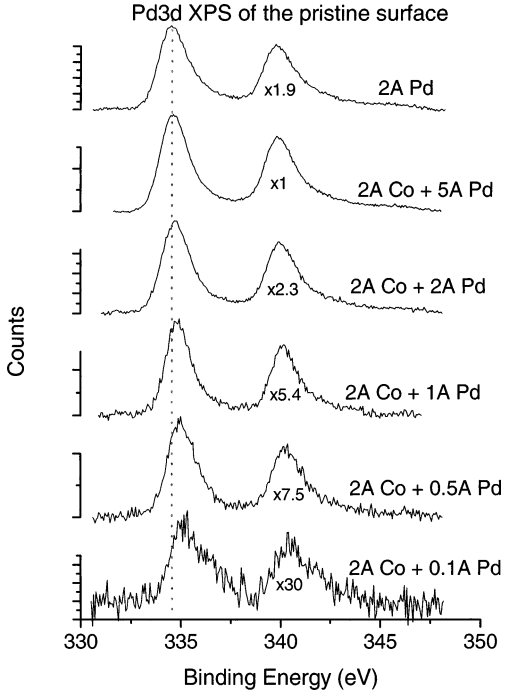

Figure 8. XPS spectra of the Pd 3d level at various Pd-shell coverages on an original 2 Å Co.

orbitals can be more significant than the net charge transfer between the two different metals;[50] thus, describing the bimetallic interaction as a charge-transfer is inadequate.

Figures 8 and 9 show XPS spectra of the Pd 3d and Co 2p levels for various Pd-shell coverages on top of 2 Å Co. At 0.1 Å Pd shell-coverage, there is a 0.4 eV shift of the Pd 3d level to higher binding energy relative to the pure Pd particles which decreases at higher Pd coverage. Again, the influence of the underlying Co core is greatest on a smaller number of Pd atoms in the shell. There is essentially no shift of the Co 2p level with varying amounts of Pd-shell coverage. A lack of shift for the core-metal when a shell is added is not surprising, though it is unclear why it differs from the case where Pd forms the core. Pd has a strong tendency to segregate to the surface of Pd−Co alloys,[51,18] suggesting that some intermixing may occur

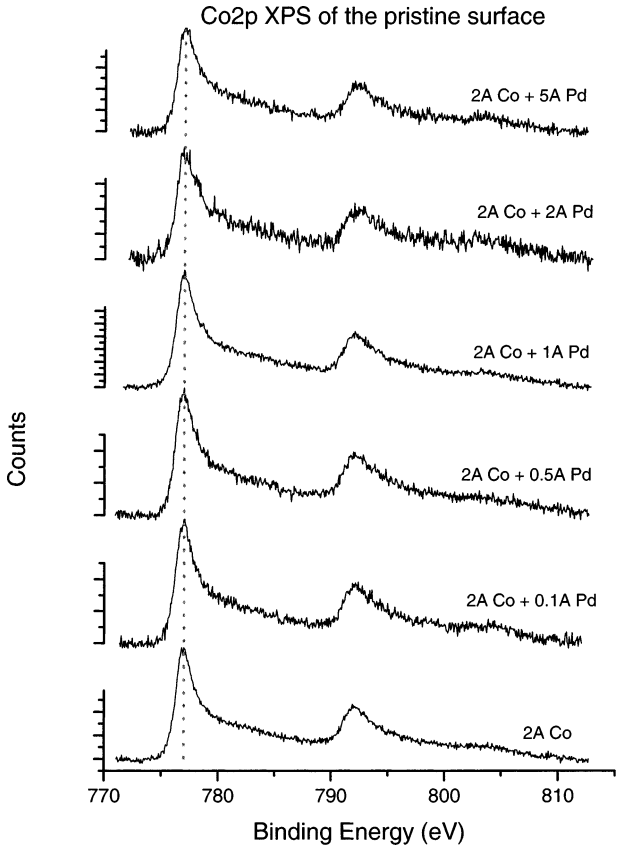

Figure 9. XPS spectra of the Co 2p level at various Pd-shell coverages on an original 2 Å Co.

in the case of a Co shell on top of Pd, accounting for the BE shift of Pd. For the reverse order, where Pd forms a shell over Co, segregation of Co to the surface should not occur, and thus no BE shift is expected.

Finally, a comparison between the Pd−Co bimetallic model catalysts studied here can be made with catalysts prepared in solution by the sol−gel method. A synergism for CO hydrogenation at a Co/Pd ratio of 2 has been observed for Co−Pd catalysts prepared by the sol−gel technique and activated in hydrogen at 400 °C.[9] Pd has been shown to segregate to the surface of Co−Pd alloys above 300 °C;[18,51] thus we would expect the CO hydrogenation reaction[9] to take place on particles of Co covered with Pd. The analogous composition for our model catalyst is 2 Å Co with subsequent deposition of 1 Å Pd. Interestingly, this is the composition where there is almost enough Pd to fully cover the Co particles, but not enough to fully block all the Co-atop sites. Further, the maximum shift in the CO binding energy is observed at this composition (Figure 3). It is possible that the direct hydrogenation of CO is facilitated at the Co-atop site in the close proximity of Pd atoms. Whether this results from a spill-over of H-atoms from the neighboring Pd-site or the electronic influence of Pd on Co needs further investigation.

Conclusions

The fundamental properties of Co−Pd bimetallic particles supported on a thin alumina film have been investigated using STM, CO-TPD, and XPS. Sequential deposition of Co and Pd results in a core−shell structure, where the second metal deposited forms the shell. While subsequently deposited Pd nucleates only on top of Co particles, subsequently deposited Co nucleates both at point defects and on top of Pd particles, due to a stronger metal−substrate interaction. CO has been used as a probe molecule in TPD measurements to characterize the binding sites of the bimetallic Co−Pd particles. The binding energy of CO to both Pd and Co sites is lowered by the presence of the other metal. CO binds preferentially to Co-atop sites and Pd 3-fold hollow sites; the Co-atop sites are better preserved at various bimetallic compositions because they are statistically less vulnerable than the Pd 3-fold hollow sites. A shift in the Pd 3d level to higher binding energy concurrent with a shift in the Co 2p level to lower binding energy suggests a net polarization of charge or redistribution of d-band states in the bimetallic particles.

Acknowledgment. We thank V. Matolin (Prague) and T. Risse (FHI Berlin) for fruitful discussions. Support for this work was provided by the Max-Planck Society and the Deutsche Forschungsgemeinschaft. A.C. thanks the Humboldt Foundation for a fellowship.

References and Notes

(1) Weissermel, K.; Arpe, H.-J. *Industrial Organic Chemistry*, 3rd ed.; VCH: Weinheim, Germany, 1997.
(2) Guczi, L.; Hoffer, T.; Zsoldos, Z.; Zyade, S.; Maire, G.; Garin, F. *J. Phys. Chem.* **1991**, *95*, 802.
(3) Guczi, L. *Catal. Lett.* **1990**, *7*, 205.
(4) Niemantsverdriet, J. W.; Loiuwers, P. A.; Groudelle, J. v.; Kraan, A. M. v. d.; Kampers, F. W. H.; Koningsberger, D. C. In *Proceedings, 9th International Congress on Catalysis, Calgary, 1988*; Chem. Inst. Canada: Ottowa, 1988; Vol. 2; p 674.
(5) Woo, H. S.; Fleisch, T. H.; Foley, H. C.; Uchiyama, S.; Delgass, W. N. *Catal. Lett.* **1990**, *4*, 93.
(6) Guczi, L.; Borko, L. *Catal. Today* **2001**, *64*, 91.
(7) Guczi, L.; Borko, L.; Schay, Z.; Bazin, D.; Mizukami, F. *Catal. Today* **2001**, *65*, 51.
(8) Tsubaki, N.; Sun, S.; Fujimoto, K. *J. Catal.* **2001**, *199*, 236.
(9) Guczi, L.; Schay, Z.; Stefler, G.; Mizukami, F. *J. Mol. Catal. A* **1999**, *141*, 177.
(10) Gimenez, F.; Chapon, C.; Henry, C. R. *New J. Chem.* **1998**, *22*, 1289.
(11) Giorgio, S.; Chapon, C.; Henry, C. R. In *Metal Clusters in Chemistry*; Braunstein, P., Oro, L. A., Raithby, P. R., Eds.; Wiley-VCH: Weinheim, 1999.
(12) Mallat, T.; Petro, J.; Szabo, S.; Sztatisz, J. *J. React. Kinet. Catal. Lett.* **1985**, *29*, 353.
(13) Mallat, T.; Petro, J.; Szabo, S.; Marczis, L. *J. Electroanal. Chem.* **1986**, *208*, 169.
(14) Mallat, T.; Szabo, S.; Petro, J. *J. Acta Chim. Hung.* **1987**, *124*, 147.
(15) Mallat, T.; Szabo, S.; Petro, J.; Mendioroz, S.; Folado, M. A. *Appl. Catal.* **1989**, *53*, 29.
(16) Idriss, H.; Diagne, C.; Hindermann, J. P.; Kinnemann, A.; Barteau, M. A. In *Proceedings, 10th International Congress on Catalysis, Budapest, 1992*; Guczi, L., Solymosi, F., Tetenyi, P., Eds.; Elsevier: Budapest, 1992; Vol. Part C.; p 2119.
(17) Kapoor, M. P.; Lapidus, A. L.; Krylova, A. Y. In *Proceedings, 10th International Congress on Catalysis, Budapest, 1992*; Guczi, L., Solymosi, F., Tetenyi, P., Eds.; Elsevier: Budapest, 1992; Vol. Part C.; p 2741.
(18) Juszczyk, W.; Karpinski, Z.; Lomot, D.; Pielaszek, J.; Paal, Z.; Stakheev, A. Y. *J. Catal.* **1993**, *142*, 617.
(19) Noronha, F. B.; Schmal, M.; Nicot, C.; Moraweck, B.; Frety, R. *J. Catal.* **1997**, *168*, 42.
(20) Noronha, F. B.; Schmal, M.; Frety, R.; Bergeret, G.; Moraweck, B. *J. Catal.* **1999**, *186*, 20.
(21) Bischoff, S.; Weight, A.; Fujimoto, K.; Lucke, B. *J. Mol. Catal. A* **1995**, *95*, 259.
(22) Ruff, M.; Frey, S.; Gleich, B.; Behm, R. J. *Appl. Phys. A* **1998**, *66*, S513.
(23) Gleich, B.; Ruff, M.; Behm, R. J. *Surf. Sci.* **1997**, *48*, 386.
(24) Liu, P.; Norskov, J. K. *Phys. Chem. Chem. Phys.* **2001**, *3*, 3814.
(25) Sinfelt, J. H. *Bimetallic Catalysts*; Wiley: New York, 1983.
(26) Rodriquez, J. A.; Kuhn, M. *Surf. Sci.* **1996**, *365*, L669.
(27) Hammer, B.; Norskov, J. K. *Adv. Catal.* **2000**, *45*, 71−129.
(28) Campbell, C. T. *Annu. Rev. Phys. Chem.* **1990**, *41*, 775.
(29) Guo, X.; Yates, J. T. *J. Chem. Phys.* **1989**, *90*, 6761.

(30) Giessel, T.; Schaff, O.; Hirschmugl, C. J.; Fernandez, V.; Schindler, K. M.; Theobald, A.; Bao, S.; Lindsay, R.; Berndt, W.; Bradshaw, A. M.; Baddleley, D.; Lee, A. F.; Lambert, R. M.; Woodruff, D. P. *Surf. Sci.* **1998**, *406*, 90.
(31) Tushaus, T.; Berndt, W.; Conrad, H.; Bradshaw, A. M.; Persson, B. *Appl. Phys. A* **1990**, *51*, 91.
(32) Ramprasad, R.; Glassford, K. M.; Adams, J. B.; Masel, R. I. *Surf. Sci.* **1996**, *360*, 31−42.
(33) Frank, M.; Baeumer, M. *Phys. Chem. Chem. Phys.* **2000**, *2*, 3723.
(34) Hansen, K. H.; Worren, T.; Stempel, S.; Laegsgaard, E.; Baeumer, M.; Freund, H.-J.; Besenbacher, F.; Stensgaard, I. *Phys. Rev. Lett.* **1999**, *83*, 4120.
(35) Dellwig, T.; Rupprechter, G.; Unterhalt, H.; Freund, H.-J. *Phys. Rev. Lett.* **2000**, *85*, 776.
(36) Dellwig, T.; Hartmann, J.; Libuda, J.; Meusel, I.; Rupprechter, G.; Unterhalt, H.; Freund, H.-J. *J. Mol. Catal. A* **2000**, *162*, 51.
(37) Lahtinen, J.; Vaari, J.; Kauraala, K.; Soares, E. A.; Hove, M. A. V. *Surf. Sci.* **2000**, *448*, 269.
(38) Lahtinen, J.; Vaari, J.; Kauraala, K. *Surf. Sci.* **1998**, *418*, 502.
(39) Toomes, R. L.; King, D. A. *Surf. Sci.* **1996**, *349*, 1.
(40) Gu, J.; Yeo, Y. Y.; Sim, W. S.; King, D. A. *J. Phys. Chem. B* **2000**, *104*, 4684.
(41) Papp, H. *Ber. Bunsen-Ges. Phys. Chem.* **1982**, *86*, 555.
(42) Stempel, S. *Nukleation, Wachstum und Struktur kleiner metallpartikel auf einer geordneten Aluminiumoxidunterlage*; (Doctoral Dissertation): Freien Universitaet, Berlin, 1998.
(43) Jaeger, R. M.; Kuhlenbeck, H.; Freund, H.-J.; Wuttig, M.; Hoffmann, W.; Franchy, R.; Ibach, H. *Surf. Sci.* **1991**, *259*, 235.
(44) Jaeger, R. M.; Libuda, J.; Baumer, M.; Homann, K.; Kuhlenbeck, H.; Freund, H. J. *J. Elect. Spectrosc. Relat. Phenom.* **1993**, *64*−*5*, 217.
(45) Hill, T.; Mozaffari-Afshar, M.; Schmidt, J.; Risse, T.; Stempel, S.; Heemeier, M.; Freund, H.-J. *Chem. Phys. Lett.* **1998**, *292*, 524.
(46) Baumer, M.; Frank, M.; Heemeier, M.; Kuhnemuth, R.; Stempel, S.; Freund, H.-J. *Surf. Sci.* **2000**, *454*, 957.
(47) Baeumer, M.; Freund, H.-J. *Prog. Surf. Sci.* **1999**, *61*, 127−198.
(48) Stempel, S.; Baumer, M.; Freund, H. J. *Surf. Sci.* **1998**, *404*, 424.
(49) Wolter, K.; Seiferth, O.; Kuhlenbeck, H.; Baeumer, M.; Freund, H.-J. *Surf. Sci.* **1998**, *399*, 190.
(50) Rodriguez, J. A. Electronic and chemical properties of palladium in bimetallic systems: How much do we know about heteronuclear metal−metal bonding? In *The Chemical Physics of Solid Surfaces and Heterogeneous Catalysis*; Woodruff, D. P., Ed.; Elsevier: Amsterdam, 2002.
(51) Krawczyk, M.; Zommer, L.; Lesiak, B.; Jablonski, A. *Surf. Interface Anal.* **1997**, *25*, 356.